ARTICLE

Direct and Inverse Auger Processes in InAs Nanocrystals: Can the Decay Signature of a Trion Be Mistaken for Carrier Multiplication?

Marco Califano*

Institute of Microwaves and Photonics, School of Electronic and Electrical Engineering, University of Leeds, Leeds LS2 9JT, United Kingdom

ABSTRACT A complete and detailed theoretical investigation of the main processes involved in the controversial detection and quantification of carrier multiplication (CM) is presented, providing a coherent and comprehensive picture of excited state relaxation in InAs nanocrystals (NCs). The observed rise and decay times of the 1S transient bleach are reproduced, in the framework of the Auger model, using an atomistic semiempirical pseudopotential method, achieving excellent agreement with experiment. The CM time constants for small core-only and core/shell nanocrystals are obtained as a function of the excitation energy, assuming an impact-ionization-like process. The resulting lifetimes at energies close to the observed CM onset are consistent with the upper limits deduced experimentally from PbSe and CdSe samples. Most interestingly, as the Auger recombination lifetimes calculated for charged excitons are found to be of a similar order of magnitude to those computed for biexcitons, both species are expected to exhibit the fast decay component in NC population dynamics so far attributed exclusively to the presence of biexcitons and therefore identified as the signature of CM occurrence in high-energy low-pump-fluence spectroscopic studies. However, the ratio between trions and biexcitons time constants is found to be larger than the typical experimental accuracy. It is therefore concluded that, in InAs NCs, it should be experimentally possible to discriminate between the two species and that the origin of the observed discrepancies in CM yields is unlikely to lay in the presence of charged excitons.

KEYWORDS: carrier multiplication · InAs nanocrystals · Auger processes · pseudopotential method · excited state relaxation

The most promising single mechanism that, if fully exploited, could greatly enhance the performance of next generation photovoltaic devices, with potentially revolutionary consequences for the efficiency with which solar power can be harnessed, is carrier multiplication (CM).[1] In this process multiple electron−hole (e−h) pairs are generated in semiconductor nanocrystals (NCs) by the absorption of single photons, owing to an efficient utilization of the photon energy in excess of the NC band gap. CM therefore would allow the conversion of solar energy of a broader spectrum and at the same time reduce the detrimental heat generation associated with conventional conversion, where each absorbed photon generates a single e−h pair, regardless of its energy.

Efficient CM has been observed in NCs of different materials (PbSe,[2−4] CdSe,[5,6] PbS,[2,4,7] PbTe,[8] Si,[9] and InAs);[10,11] however, subsequent reports on the absence of detectable CM in CdSe, CdTe,[12] and InAs (where some authors[13,14] even refuted their own earlier results),[10] have cast serious doubts on the very existence of such effect, at least in those materials. Although most recent measurements in PbSe[15−17] and PbS,[15] confirmed the occurrence of CM in the lead salts, albeit with significantly lower efficiencies than previously estimated, the whole issue has remained highly controversial. The inherent complexity of the detection and quantification of CM in NCs, whose subtleties have been recently discussed in refs.13 and 16, is to blame for that. Regardless of the technique used for the investigation (time-resolved transient absorption,[3] time-correlated single photon counting,[12,18] and terahertz time-domain spectroscopy[10] are the main tools employed to this end), the feature that allows CM to be observed is the fundamental difference in decay between single and multiple excitons where slow radiative decay (≥ns) of the former is contrasted by ultrafast (∼ps) Auger recombination (AR, Figure 1a) of the latter. AR is however a *three* particle process in which the recombination energy of an e−h pair is not emitted as a photon but, due to a confinement-enhanced Coulomb interaction, is efficiently transferred nonradiatively to *an additional* carrier (a hole in Figure 1a) which is promoted to a highly excited state. As a consequence, the detection of a fast decay component does not necessarily imply the presence of a multiexciton, but could also be consistent with the presence of a

*Address correspondence to m.califano@leeds.ac.uk.

Received for review May 6, 2009 and accepted August 10, 2009.

Published online August 18, 2009. 10.1021/nn900461f CCC: $40.75

charged exciton or trion (*i.e.*, two electrons and a hole or two holes and an electron, see Figure 1c,d). In the latter case no CM would have taken place, despite the presence of a fast decay component. This scenario was suggested by some authors[17] as a possible explanation for the discrepancies observed between CM yields estimated in different experiments and could be the result of NC photoionization, which could be caused by the high energy (usually of the order of several times the NC band gap) of the pump photon required to initiate CM. Another closely related aspect that could play an important role to explain the discrepancies in the measured CM efficiencies is the surface passivation chemistry[19] (and its interplay with charged states),[20] whose effects on carrier dynamics are still poorly understood. It follows that the first steps toward understanding whether CM is a real phenomenon or a detection artifact are to investigate (i) whether the fast decay observed in the band-edge exciton bleach is indeed due to AR and (ii) what excitonic states can be associated with it. This investigation is also crucial in the light of possible photovoltaic applications, as AR represents the main (*i.e.*, most efficient) carrier loss channel that competes with charge separation in a solar cell. In other words, in order for the CM potentiality to be exploited in any energy conversion device, the carriers need to be separated in time scales that are small compared to the AR lifetime, otherwise they will recombine and the CM benefit will be lost. For similar reasons any efficient nonradiative decay also represents a major obstacle for the application of NCs in lasing, as radiative recombination is several orders of magnitude slower than both Auger electron cooling (AC, Figure 1e) and AR.

The next aspect of CM one may wish to consider is its time constant. The current experimental estimates are based on the 1S transient-absorption signal buildup dynamics.[3] As electron Auger intraband relaxation (where an excited electron relaxes to its ground state by transferring its excess energy nonradiatively to a hole and exciting it to deep valence band states, see Figure 1e), is the mechanism that controls the signal buildup in the absence of CM, a theoretical investigation of this process may prove insightful.

Another important aspect related to CM, which crucially contributes to the determination of the solar cell efficiency, is the threshold for CM onset, experimentally defined[2] as the lowest pump photon energy associated with the detection of a biexciton (in CM the carrier distribution is in fact characteristically nonpoissonian[21] and depends on the excitation *energy* rather than its *intensity*). As the energy conversion efficiency for a single absorber with a single energy gap is inversely proportional to the CM threshold, the natural question to ask is what material will exhibit the lowest threshold. On the basis of simple effective-mass considerations applied to a two-band model,[22] Schaller et al.[5,11] showed the photon energy in excess of the NC band gap $\Delta E = \hbar\omega - E_g$ to be unequally divided between the photogenerated electron and hole according to

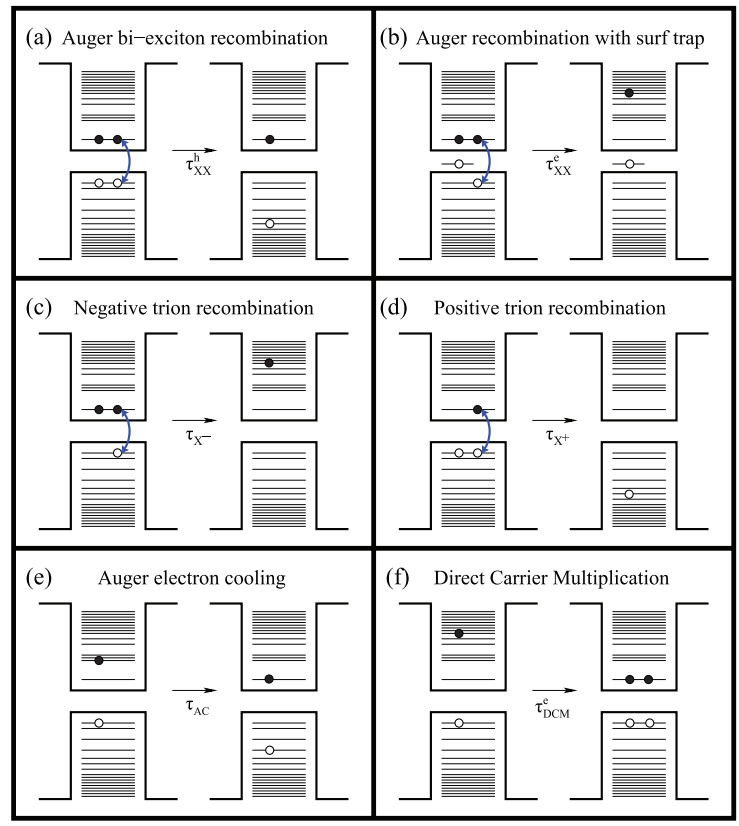

Figure 1. Schematics of the Auger processes considered in this work: (a) Auger biexciton recombination with hole excitation, (b) Auger biexciton recombination with electron excitation in the presence of a surface hole trap state, (c) Auger negative trion recombination, (d) Auger positive trion recombination, (e) Auger electron cooling, (f) hot-electron-initiated direct carrier multiplication (DCM).

$$\frac{\Delta E_e}{\Delta E_h} = \frac{m_h}{m_e} \quad (1)$$

(where ΔE_e and ΔE_h are the excess energies in the conduction and valence band, respectively, and $\Delta E_e + \Delta E_h = \Delta E$), giving an inverse dependence on the carrier effective mass. Because of the large difference between electron and hole effective masses in InAs, where $m_h/m_e = 17$,[23] eq 1 would predict over 94% of the excess energy to be transferred to the electron in NCs made of this material. InAs NCs are therefore expected to exhibit some of the lowest attainable threshold energies compatible with energy conservation, and recent experimental data[10,11] seem to confirm this expectation.

From energy conservation considerations, the minimum photon energy required for CM to take place (the CM threshold energy $\hbar\omega_{CM}$) can be expressed within this simple model[11] as

$$\hbar\omega_{CM} = \left(2 + \frac{m_e}{m_h}\right)E_g \quad (2)$$

Equation 2 therefore provides a simple explanation for the observed *material* dependence of the *normalized*

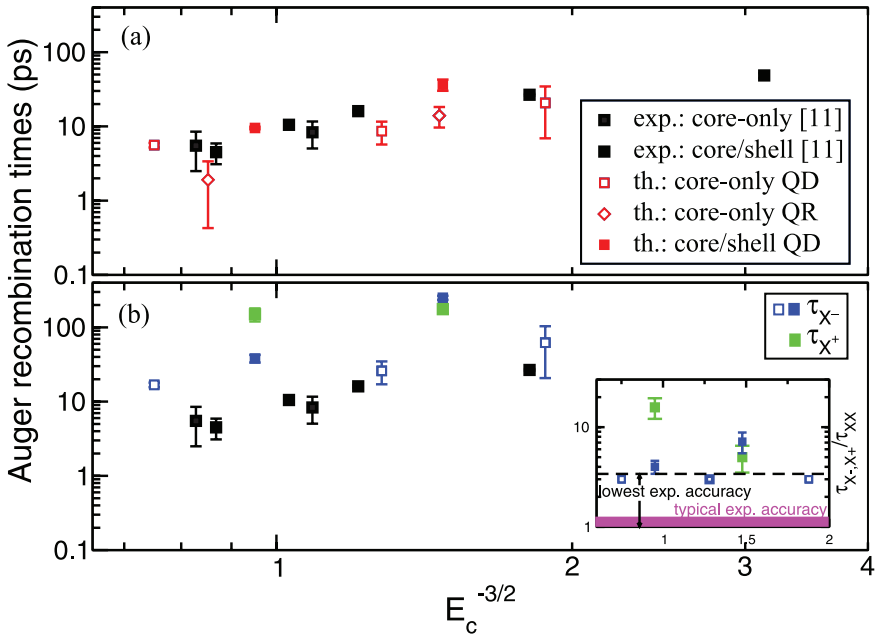

Figure 2. Auger recombination lifetimes (in ps) as a function of the NC confinement energy $E_c = E(1S) - E_{gap}^{bulk}$.[11] The theoretical results obtained here for (a) τ_{XX} (red symbols), and (b) τ_{X^-} (blue symbols) and τ_{X^+} (green symbols), in core-only spherical (empty squares) and elongated (empty red diamonds) NCs and core/shell spherical dots (solid squares) are compared with the experimental data of ref 11 (black symbols, empty squares for core-only and solid squares for core/shell structures). Inset: the ratio $\tau_{X^-,X^+}/\tau_{XX}$ quantifies the degree of similarity between the decay times of trions and biexcitons.[40] The dashed line marks the lower limit of experimental accuracy in ref 11, obtained for small core-only samples, whereas the magenta sector indicates the typical accuracy reached for core/shell structures in the experiments (see text for details). The error bars in the theoretical data in all panels account for a 10% size distribution in the experimental samples.

CM threshold energy $\hbar\omega_{CM}/E_g$, which decreases from PbS and PbSe (~3),[7] to CdSe (~2.5),[5] to InAs (~2 for large NC sizes).[11] However, unlike in the case of PbSe, PbS, and CdSe NCs where, according to eq 2, a fixed CM onset was observed, the normalized CM threshold in InAs NCs shows a strong size dependence[11] which is not accounted for in eq 2 and has remained so far unexplained.

We will concentrate here on excited state decay dynamics in InAs NCs, trying to shed light on some of the above-mentioned issues. The results of a detailed theoretical investigation based on the pseudopotential method, presented here, show that (i) the observed rise times of the 1S exciton bleach[11] and the biexciton lifetimes extracted from pump-intensity-dependent transient absorption dynamics[11] can be reproduced by assuming Auger-like carrier relaxation processes in analogy to the case of CdSe NCs;[24,25] (ii) although a fast decay in the 1S exciton bleach at early times can also be consistent with the presence of charged excitons and not only multiple excitons, the decays of the two species should be easily distinguishable within the experimental accuracy, due to a difference of a factor of 3 or more between their time constants; (iii) due to the prevalent p symmetry of the envelope functions of the degenerate valence band maximum (VBM) and VBM-1 states in InAs NCs,[26,27] the band edge (1S) absorption occurs from the (mainly) s degenerate states VBM-2 and VBM-3, and therefore when the hole recombines with the electron *via* AR it may still occupy such excited states, especially if the s−p energy separation Δ_{sp}^h does not match available phonon energies; (iv) most importantly, while as a consequence of the optical selection rules the minimum energy absorbed by the system is $E(1S) = E(e_1,h_{1,2}) + \Delta_{sp}^h$, such rules do not apply to Coulomb-mediated interactions like CM which can be initiated by a carrier with energy $E(e_1,h_{1,2}) = E(1S) - \Delta_{sp}^h$; this feature could explain part of the puzzling size-dependence observed in $\hbar\omega_{CM}$ in terms of the size dependence of Δ_{sp}^h; (v) the CM time constant calculated for a R = 14.6 Å NC is of the order of a few tens of femtoseconds for the CM onset energies observed experimentally, consistent with the experimental upper bound estimated for PbSe and CdSe,[3] and with previous theoretical estimates.[50]

RESULTS AND DISCUSSION

Auger Processes in Core-Only and Core/Shell Structures. Electron intraband relaxation times were measured in InAs/CdSe core/shell structures, whereas biexciton recombination rates were also measured in InAs core-only samples.[11] As AR is supposed to receive large contributions from the NC surface,[6,25,32] very different lifetimes would be expected for the two sets (core-only and core/shell) of experimental samples.

Despite exhibiting large quantitative and qualitative differences in single-exciton excited-state decay (single-exponential *vs* biexponential relaxation with PL lifetimes differing by nearly 3 orders of magnitude),[11] and large differences in quantum yield, all suggestive of a different passivation quality and of the different involvement of the surface in the two cases (with carrier trapping[11] presumably playing a substantial role in core-only NCs), remarkably the measured biexciton recombination times in core/shell and core-only samples were indistinguishable, within experimental error, as it was the case for CdSe NCs, where TOPO- and ZnSe-capped[33] samples, in one case, and TOPO- and ZnS-capped[24] NCs, in another case, exhibited identical biexciton decay times. The reasons behind this effect are still controversial[6,24,33] and a quantitative interpretation had not been attempted since very recently, when it was found[34] that in CdSe when a hole is trapped at the NC surface (Figure 1b), due to the reduced overlap between the carriers' wave functions, the hole contribution to the AR rate (τ_h^{-1}) becomes much smaller than the electron contribution τ_e^{-1} (see Method section for

a detailed definition of these rates), so that $\tau_{XX} \approx \tau_e$. The results presented in Figure 2, where the values of τ_e calculated for core-only samples (empty red squares in panel a) are in excellent agreement with the measured decay times,[11] seem to suggest that this may be the case for InAs NCs as well.

It has been recently suggested,[35] based on a detailed theoretical analysis of the observed optical spectra,[36−38] that slightly elongated NCs (quantum rods, QRs) with aspect ratios between the two main diameters of the order of about 1.2 may be present in the experimental (core-only) samples synthesized according to the procedure, detailed by Guzelian *et al.*,[39] followed by Schaller *et al.*[11] for the synthesis of their core-only NCs. Interestingly the values of τ_e calculated for such structures (empty red diamonds in Figure 2a) are also in good agreement with experiment.

The growth of a CdSe shell leads to a ∼100-fold increase in the quantum yield[11] suggesting the achievement of a better passivation and the removal of most surface trap states. Because of the bulk band alignment at the InAs/CdSe interface,[42] yielding a small conduction band offset (0.46 eV) contrasted by a substantial offset for the valence band (0.92 eV), the presence of a CdSe shell is believed[43] to have opposite effects on electrons and holes, allowing penetration into the shell region by the former while confining the latter to the core. This hypothesis is supported by the observation[11,43] of a red shift in the lowest-energy absorption feature (usually referred to as the 1S exciton feature) after the growth of the CdSe shell, interpreted[43] as an indication of an increase in the effective radius of the NCs, due to the reduction of the electron confinement.

To simulate the effect of the presence of a ∼2 ML[11] electron-deconfining, hole-confining CdSe shell in InAs NCs of core radius R, the Auger decay rates were calculated using the conduction band states relative to structures with radius $R + \delta R$, (where $\delta R \approx 5$ Å is the shell thickness) and the valence band states obtained for NCs with radius R. To assess how realistic this choice may be, the red shift calculated within this model for a 14.6 Å core with a 5.4 Å shell (176 meV) was compared with the experimental value[43] relative to the growth of a 5 Å shell (∼180 meV), yielding excellent agreement. Further support for the model comes from the observation that the measured Stokes shift between the 1S absorption feature and the PL band remains approximately constant upon growth of the CdSe shell.[11] According to our calculations,[27,41] due to optical selection rules, such a shift is mainly due to the energy separation $\Delta^h_{s,p}$ between the degenerate (VBM,VBM-1) states, having prevalent p symmetry, and the next degenerate (VBM-2,VBM-3) states having main s symmetry.[44] In our model this separation remains unchanged upon growth of the shell, in agreement with experiment.

The AR times calculated for core/shell structures are in good agreement with the biexciton lifetimes measured in InAs/CdSe[11] structures for all sizes considered (see Figure 2a), indicating once more that our core/shell model is suitable to describe the electronic properties of InAs/CdSe NCs. Most importantly, however, the calculated AR lifetimes of positively (Figure 1d) and negatively (Figure 1c) charged excitons are found to be of a similar order of magnitude to those relative to biexcitons (Figure 2b), implying that similar signatures are to be expected in the early times population dynamics of the two species. To make the comparison more quantitative, the inset of Figure 2b displays the ratios τ_{X^-}/τ_{XX} and τ_{X^+}/τ_{XX}, showing that, in core/shell NCs, the trion lifetime is at least four times that of the biexciton for the sizes considered here (large ratios between the lifetimes of negative trions and biexcitons were also recently found by Jha and Guyot-Sionnest in CdSe/CdS core/shell NCs.)[45] This ratio reduces to three for negative trions in core-only NCs in which case, however, due to the substantial presence of surface states,[11] the relationship $\tau_{XX} \approx \tau_e$ was assumed to hold.

The question is now whether this difference can be detectable experimentally. According to the data presented in Figure 2f of ref 11, the worst experimental accuracy is 54% (*i.e.*, 5.5 ± 3 ps) and was found for the smallest (core-only) NC. This means that its lifetime, ranging from 2.5 to 8.5 ps, exhibits a difference of a factor of 3.4 between its extreme values (dashed line in the inset of Figure 2b). Such difference is of a factor of 2.3 for the other core-only NC, but is always less than a factor of 2 (typically of the order of 1.1−1.2, as shown by the magenta area in the inset of Figure 2b) for all the other (core/shell) nanostructures investigated in ref 11, suggesting that the factor of 4 (or more) difference found between the decay time constants calculated for trions and biexcitons in the case of core/shell samples should be easily detectable experimentally. In the case of core-only samples, however, the experimental accuracy could be insufficient to discriminate between the presence of charged and neutral NCs, at least for small dots. This result therefore suggests that the CM yields deduced in ref 11 for core/shell NCs are not likely to have been affected by the presence of trions. Although the same may be true for other experiments, this conclusion cannot be easily generalized to the large variations in CM yields observed in different experimental settings and different structures/materials, as the calculations presented here are specific for InAs core-only and core/shell NCs.

Size Dependence of the CM Onset in InAs NCs. Interestingly, it was found that by considering initial states where the hole occupied its degenerate ground state $h_{1,2}$ (VBM,VBM-1) it was not possible to reproduce the observed AR lifetimes. As a consequence of the prevalent p symmetry[26,27] of this state, mentioned above, when the NCs are photoexcited, the band edge 1S optical ab-

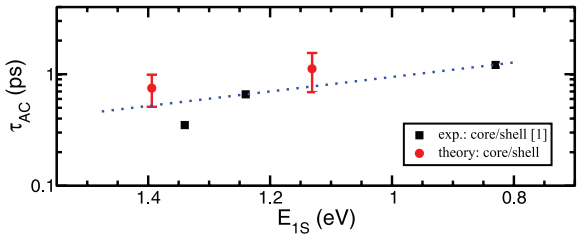

Figure 3. Comparison between calculated (red circles) and observed (black squares) Auger cooling times in InAs/CdSe core/shell NCs as a function of the emission energy *E*(1S). The dotted line is a guide to the eye.

sorption occurs from the degenerate, mainly s states, $h_{3,4}$ (VBM-2,VBM-3), and therefore when AR takes place the hole may still occupy such excited states, especially if the sp energy separation Δ^h_{sp} in the valence band does not match available phonon energies. The colored squares in Figure 2 were obtained precisely by selecting initial configurations with the hole in one of the s states.

This feature of the VB in InAs NCs has important implications for CM and could explain part of the puzzling size dependence of the CM threshold observed recently.[11] For a *qualitative* understanding of the reasons behind this effect, we shall employ the very same simple and intuitive effective mass arguments that Schaller *et al.* used to explain the material dependence of the CM threshold. Let us start by defining the observed optical gap $E(1S) = E(e_1,h_{1,2}) + \Delta^h_{sp}$ and consequently the photon excess energy $\Delta E = \hbar\omega - E(1S)$. From eq 1 we can derive

$$\Delta E_e = \Delta E \frac{m_h}{m_e + m_h} \tag{3}$$

The CM threshold in ref 11 was derived from the condition

$$\max(\Delta E_e, \Delta E_h) = E_g \tag{4}$$

However, in eq 4 $E_g = E(\text{CBM,VBM})$, which for InAs NCs yields $E_g = E(e_1,h_{1,2}) = E(1S) - \Delta^h_{sp}$. In fact in CM the excitation of a VB electron (or, to be more general, the coupling between single-exciton and multiexciton states) occurs *via* Coulomb interaction, which is not constrained by the optical selection rules that determine E(1S). Combining eqs 3 and 4 we get

$$\hbar\omega_{CM} = \left(2 + \frac{m_e}{m_h}\right)E(1S) - \Delta^h_{sp}\left(1 + \frac{m_e}{m_h}\right) \tag{5}$$

which contains the desired size dependence through the sp splitting in the VB [note that the CM threshold is usually expressed in units of *E*(1S)]. According to the values calculated here for *E*(1S) and Δ^h_{sp}, this simple model would predict a nonmonotonic trend with size for $\hbar\omega_{CM}$: the highest value for the CM threshold energy is obtained for the smallest NC considered; the lowest for the medium size NC, and an intermediate value for the largest NC, in agreement with what was observed in ref 11. It should be emphasized here once again that this is only a simple model, that completely neglects the complexity of the band structure of real NCs and any interactions between charge carriers. As such it can only yield a qualitative explanation of the observed trends for size and material dependence of the CM threshold energy.

Another implication of eq 5 is that it should be possible to achieve a CM threshold closer to the *apparent* energy conservation limit of $2E_g = 2E(1S)$, although, if *E*(1S) is expressed in terms of the energy gap relevant to CM, $E(e_1,h_{1,2})$, the threshold is

$$\hbar\omega_{CM} = \left(2 + \frac{m_e}{m_h}\right)E(e_1, h_{1,2}) + \Delta^h_{sp} \tag{6}$$

farther away from the real energy conservation limit of $2E_g = 2E(e_1,h_{1,2})$.

CM Time Constant and 1S Population Buildup. One of the most controversial issues related to CM is the determination of its time constant: according to the different models proposed in the literature to date, it can range anywhere from 0 (*i.e.*, an instantaneous process, as proposed by Schaller *et al.*)[3] to a few hundreds of femtoseconds.[4,46,47] Experiments[3] have set an upper limit for it at about 400 fs in CdSe and PbSe (with the experimentalists speculating CM to occur on time scales that are even shorter than their wavelength-dependent time resolution of 50−200 fs),[3] based on the comparison of the buildup dynamics of the lowest 1S electron state in transient absorption measurements obtained for different excitation energies, above and below the CM threshold. No equivalent study has been carried out so far for InAs NCs, for which electron intraband relaxation times are available only for excitation energies below $\hbar\omega_{CM}$.[11]

To gain further credibility for our method, we therefore assessed its capability to also reproduce the observed electron lifetimes for low excitation energies. The electron 1P-to-1S state relaxation times calculated, as explained in the Methods section, assuming a Coulomb-mediated decay (*i.e.*, Auger cooling, Figure 1e) in core/shell structures are in good agreement with the experimental data[11] (see Figure 3) and confirm once more[25,48,49] the suitability of the semiempirical pseudopotential method for the study of excited state relaxation dynamics in semiconductor NCs.

In light of the above results we proceeded to the evaluation of the CM time constant. To date there is no general consensus regarding the underlying mechanism responsible for CM, and different hypotheses have been proposed so far in the literature.[3,46,47,50,52,53] In this work we will follow our original proposition[52,53] of an impact-ionization-like process, which we termed direct carrier multiplication or DCM. According to the DCM model, the absorption of a high-energy photon

with $\hbar\omega > 2E_g$ creates a highly excited e−h pair. If the excess energy of one of the carriers (due to its lighter effective mass, usually the electron) exceeds E_g then, upon relaxation of the carrier to its band edge, such energy can be transferred efficiently, *via* a Coulomb-mediated transition, to a valence electron, promoting it across the band gap and creating an additional e−h pair (Figure 1f). As pointed out by many authors,[3,46,47,50] in the impact ionization model the matrix elements involved in the calculation of the CM lifetime are the same as those used for calculating the AR time, the only *crucial* difference being the inversion between initial and final states in the two processes

$$\frac{1}{\tau_{DCM}} = \frac{2\pi}{\hbar}\sum_f |\langle X_i|W|XX_f\rangle|^2\delta(E_i - E_f) \quad (7a)$$

$$\frac{1}{\tau_{AR}} = \frac{2\pi}{\hbar}\sum_f |\langle XX_i|W|X_f\rangle|^2\delta(E_i - E_f) \quad (7b)$$

Indeed DCM is the inverse process of AR (see Figure 1a,f).

Given the excellent agreement with experiment achieved for the AR lifetimes, the pseudopotential method is therefore ideally suited for the evaluation of the CM time constant. An interesting property of these matrix elements is their energy independence, that is, the fact that, as shown by Delerue *et al.*,[50] they are almost constant over a wide range of energies of the initial DCM states. This property was used by Franceschetti *et al.*[47] to deduce the DCM rates in PbSe NCs as a function of energy starting from the experimentally measured AR lifetime. We will exploit it here to calculate the DCM time constant as a function of the photon energy for an InAs NC with $R = 14.6$ Å, (the size for which the agreement with experiment was best and which was small enough to allow the direct calculation of all bound states) starting from our calculated matrix element for AR. To do that we calculated the 1e−1h and 2e−2h density of states (DOS) $\rho_X(E) = \delta(E - E_f^X)$ and $\rho_{XX}(E) = \delta(E - E_f^{XX})$, only including states that can be connected by Coulomb interaction,[51] that is, those states that differ by no more than three single particle states, as pointed out by Luo *et al.*[54] (although they found the ratio ρ_{XX}/ρ_X calculated using density of states that account for the correct Coulomb coupling to be generally similar, in a wide range of materials, to that obtained using density of states that consider all possible states). Finally, using eq 7, the DCM time constant could be simply obtained as

$$\tau_{DCM}(E) = \tau_{AR}\frac{\rho_X(2E_g)}{\rho_{XX}(E)} \quad (8)$$

When applied to CdSe NCs this procedure yielded[55] results consistent with those obtained using the DCM matrix elements directly calculated according to refs 52 and 53. The resulting DCM time constant, displayed as a function of the excitation energy (normalized by E_g), is presented in Figure 4, showing that DCM can be as fast as few tens of femtoseconds already for excitation energies just above the observed CM onset ($E/E_g \gtrsim 2.5$[11] for a NC with similar size), consistent with previous predictions based on tight-binding calculations[50] and with the shortest estimates of the CM time constant deduced from measurements in CdSe and PbSe NCs.[3] Recent detailed pseudopotential calculations of the distribution of the CM rates following photon absorption, performed by Rabani and Baer,[56] estimate instead an average lifetime for the exciton to biexciton transition of about 17 ps at $E = 2.5E_g$ in InAs NCs with $D = 31$ Å. If this decay time is used to estimate the AR lifetime by inserting it (together with the excitonic and biexcitonic DOS calculated in ref 56) into eq 8, however, a value of about 50 ps is found, which is about an order of magnitude larger than both the lifetime calculated here and that observed experimentally for similar sizes (see Figure 2). Rabani and Baer found[56] a broad distribution of exciton-to-biexciton transition rates, spanning 4−6 orders of magnitude at a given exciton energy, depending on the specific exciton considered, therefore several of the rates included in such a large range would yield good agreement with the observed AR rates, when substituted in eq 8. Nevertheless, given the large number of excitons included in Rabani and Baer's calculations it is surprising that the simple estimate based on eq 8 may yield shorter DCM lifetimes.

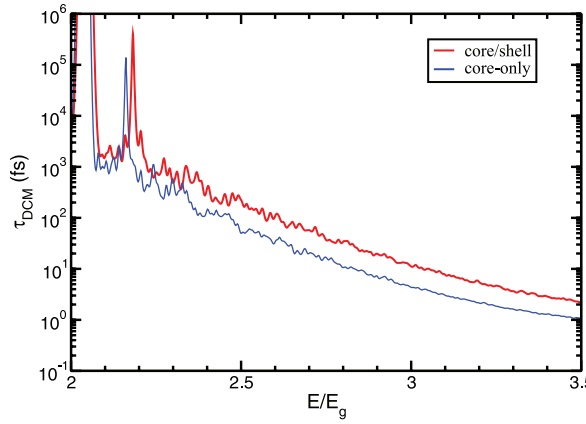

Figure 4. Calculated DCM time constant as a function of the excitation energy for InAs core-only (blue line) and InAs/CdSe core/shell NCs (red line). The value of τ_{DCM} at the CM threshold observed for such small NCs ($E/E_g \gtrsim 2.5$)[11] can be ≲50 fs for core-only samples and ≲180 fs for core/shell NCs. The large oscillations near the energy conservation threshold $E/E_g = 2$, also found in previous theoretical studies,[50] are due to the low density of biexcitonic states at that energy. This effect is particularly pronounced in InAs, compared, for example, with PbSe, as the CBM is nondegenerate in this semiconductor.

The possible sources of error in our derivation (eq 8) which would have led to an underestimate of τ_{DCM} are three: (i) variable, as opposed to constant, matrix elements; (ii) an underestimate of $\rho_X(2E_g)$; (iii) an overestimate of $\rho_{XX}(E)$. Even assuming an unlikely large variation of 1 order of magnitude (not found in ref 50, but

found for the *effective* coupling in ref 56), in the matrix elements (i), our DCM lifetimes would still be more than 1 order of magnitude shorter than those calculated in ref 56. (ii) $\rho_X(2E_g)$ was obtained from the very same states included in the calculation of the AR lifetime and is therefore not likely to have been underestimated. Finally, given that in ref 56 the authors emphasize the necessity of including *all* states in order to obtain reliable estimates of the CM rates, the value of $\rho_{XX}(E)$ calculated here (iii) could only have been underestimated (but not overestimated), compared with their calculation. We conclude that it is unlikely that errors in our estimate of τ_{DCM} could explain the large discrepancy between the lifetimes reported in ref 56 and those estimated here and in ref 50.

The origin of this discrepancy may lay in the different screening assumed in the two calculations. As discussed in the Method section below, conforming to the results of recent LDA[30] and tight-binding[29] calculations, the interactions at the NC surface are assumed to be unscreened in the present work, and screened by the bulk dielectric constant in the dot interior,[25] whereas the effect of this screening was captured on average in ref 56 by employing a size-dependent dielectric constant ($\varepsilon(R)$). As the wave functions of the highly excited initial states involved in the DCM process are expected, due to the large kinetic energy associated with them, to be more localized on the NC surface than in its core, this may yield to differences in the calculated rates of the order of $\varepsilon(R)^2$ (*i.e.*, about 2 orders of magnitude, for large dots). This, together with some variability of the matrix elements with energy, could account for the discrepancy in the calculated DCM lifetimes.

CONCLUSIONS

The biexciton decay time constants and the 1P-to-1S electron relaxation lifetimes in InAs NCs of different sizes have been calculated using the atomistic semiempirical pseudopotential method and the results were found in very good agreement with recent experimental data. The calculated CM time constant reaches values of tens of fs at energies close to the observed CM onset, consistent with the upper limits experimentally estimated for CdSe and PbSe, and indicating a fast and efficient process. Finally, the large values found for the ratio between the Auger recombination times calculated for trions and biexcitons suggest that, although the observation of a fast component in the band edge exciton bleach decay at high excitation energies cannot be considered alone as a reliable indicator of the presence of biexcitons, it should be possible to experimentally determine the presence of charged NCs based on the magnitude of such component. This result, although not straightforwardly generalizable to other material systems, seems to suggest that the explanation for the observed large variability in CM yields may lay elsewhere: surface chemistry effects are the most likely candidates.

COMPUTATIONAL METHODS

The electronic structure of spherical InAs NCs with radii of 14.6, 20.0, and 25.0 Å was calculated according to the semiempirical pseudopotential method[28] following the procedure detailed in ref 27. AC and AR rates were calculated within the standard time-dependent perturbation theory according to[25]

$$1/\tau_i = \frac{2\pi}{\hbar}\sum_f |\langle i|W|f\rangle|^2 \delta(E_i - E_f) \quad (9)$$

where $|i\rangle$ and $|f\rangle$ are the initial and final Auger electronic states, with energies E_i and E_f, and W is the screened Coulomb interaction. The delta function was broadened using a Lorentzian line shape

$$\delta(E_i - E_f) = \frac{1}{\pi}\frac{(\Gamma/2)}{(E_i - E_f)^2 + (\Gamma/2)^2} \quad (10)$$

where $\hbar/\Gamma$ is the lifetime of the final states (the value used in this work is $\Gamma = 10$ meV but it was found here that Auger lifetimes are almost unaffected by variations in Γ of over 1 order of magnitude from 5 to 100 meV. Such variations only affect the results accounting for size-inhomogeneities in the experimental samples by increasing the length of the error bars in Figures 2 and 3).

As in ref 25 the AR rates τ_{XX}^{-1} were evaluated combining two contributions τ_e^{-1} and τ_h^{-1}, deriving, respectively, from the excitation of an electron, (as displayed schematically in Figure 1b for a case in which the excitation occurs in the presence of a surface hole trap state), and from the excitation of a hole (see Figure 1a), as $\tau_{XX}^{-1} = \tau_e^{-1} + \tau_h^{-1}$.

Electron and hole contributions can, in turn, be expressed in terms of the decay of a negative ($1/\tau_{X^-}$) and a positive ($1/\tau_{X^+}$) trion as $\tau_e^{-1} = 3/\tau_{X^-}$ and $\tau_h^{-1} = 2/\tau_{X^+}$, where the different values of the constants are due to the different configurations available in the two cases when the valence band maximum is 2-fold degenerate (without spin). The AR rates were obtained including (as final states) up to 32 electron (for τ_e^{-1}) and up to 37 hole levels (for τ_h^{-1}) centered around the energies $\varepsilon_{e_s} + \varepsilon_{gap}$ and $\varepsilon_{h_s} - \varepsilon_{gap}$, respectively (where $\varepsilon_{gap} = \varepsilon_{e_s} - \varepsilon_{h_s}$), whereas in the calculation of AC lifetimes 40 hole final states centered around $\varepsilon_{h_1} - \Delta\varepsilon^e_{sp}$ ($\Delta\varepsilon^e_{sp} = \varepsilon_{e_p} - \varepsilon_{e_s}$) were employed. In all cases a window of at least 160 meV (*i.e.*, at least 80 meV either side of the reference energy) was covered by the final states. Since the experiments were performed at room temperature a Boltzmann average over the initial states was considered.

Screening in Semiconductor NCs. Recent tight-binding[29] and LDA[30] calculations found that the dielectric constant of a semiconductor NC is bulk-like in the core up to a small (*ca.* 1−2 Å) distance from the surface where it decreases to 1. Accordingly, in the calculation of the Auger integrals,[31] the regional screening developed in ref 25 was adopted, where the microscopic dielectric function of the dot is expressed in terms of a core and a surface term as

$$\varepsilon^{-1}(\mathbf{r},\mathbf{r}') = \varepsilon_{out}^{-1}(\mathbf{r},\mathbf{r}') + (\varepsilon_{in}^{-1}(\mathbf{r},\mathbf{r}') - \varepsilon_{out}^{-1}(\mathbf{r},\mathbf{r}'))\, m(r)\, m(r') \quad (11)$$

In eq 11 $m(r)$ changes smoothly from 1, when r is inside the dot ($r < R_{dot} - d$), to 0, when r is outside ($r > R_{dot} + d$), yielding $\varepsilon(\mathbf{r},\mathbf{r}') = \varepsilon_{in}$ inside the dot, while $\varepsilon(\mathbf{r},\mathbf{r}') = \varepsilon_{out}$ when r, or r', or both are outside the dot (here d is chosen = 1 Å, but the choice d = 2 was found in the past[25] to give similar results). ε_{in} was therefore assumed to be equal to the bulk screening, whereas ε_{out} was

chosen equal to 1, consistently with refs 29 and 30, for core-only structures, and equal to the dielectric constant of the shell ($\varepsilon_{CdSe} = 6$) for InAs/CdSe core/shell NCs.

Acknowledgment. I would like to thank Peter Graf for kindly providing the code used for the NC passivation and for his precious help and advice in the passivation procedure. I'm also grateful to Richard Schaller for sharing his data and for insightful discussions on core/shell NCs, to Alberto Franceschetti and Alex Zunger for their valuable suggestions and comments, and to John McGuire for discussion of his results. The NanoPSE computational package developed at the National Renewable Energy Lab (Golden, CO, U.S.) was used for all the calculations performed here, thanks to Alex Zunger's permission. This work was carried out using the U.K. National Grid Service (NGS). The Royal Society is gratefully acknowledged for financial support under the URF scheme.

REFERENCES AND NOTES

1. Nozik, A. J. Quantum Dot Solar Cells. *Physica E* **2002**, *14*, 115–120.
2. Schaller, R. D.; Klimov, V. I. High Efficiency Carrier Multiplication in PbSe Nanocrystals: Implications for Solar Energy Conversion. *Phys. Rev. Lett.* **2004**, *92*, 186601-1–186601-4.
3. Schaller, R. D.; Agranovich, V. M.; Klimov, V. I. High-Efficiency Carrier Multiplication Through Direct Photogeneration of Multi-Excitons *via* Single-Exciton States. *Nat. Phys.* **2005**, *1*, 189–194.
4. Ellingson, R.; Beard, M. C.; Johnson, J. C.; Yu, P.; Micic, O. I.; Nozik, A. J.; Shabaev, A.; Efros, A. L. Highly Efficient Multiple Exciton Generation in Colloidal PbSe and PbS Quantum Dots. *Nano Lett.* **2005**, *5*, 865–871.
5. Schaller, R. D.; Petruska, M. A.; Klimov, V. I. Effect of Electronic Structure on Carrier Multiplication Efficiency: Comparative Study of PbSe and CdSe Nanocrystals. *Appl. Phys. Lett.* **2005**, *87*, 253102-1–253102-3.
6. Klimov, V. I. Mechanisms for Photogeneration and Recombination of Multiexcitons in Semiconductor Nanocrystals: Implications for Lasing and Solar Energy Conversion. *J. Phys. Chem. B* **2006**, *110*, 16827–16845.
7. Schaller, R. D.; Sykora, M.; Pietryga, J. M.; Klimov, V. I. Seven Excitons at a Cost of One: Redefining the Limits for Conversion Efficiency of Photons into Charge Carriers. *Nano Lett.* **2006**, *6*, 424–429.
8. Murphy, J. E.; Beard, M. C.; Norman, A. G.; Ahrenkiel, S. P.; Johnson, J.C.; Yu, P.; Micic, O. I.; Ellingson, R.; Nozik, A. J. PbTe Colloidal Nanocrystals: Synthesis, Characterization, and Multiple Exciton Generation. *J. Am. Chem. Soc.* **2006**, *128*, 3241–3247.
9. Beard, M. C.; Knutsen, K. P.; Yu, P.; Luther, J. M.; Song, Q.; Metzger, W. K.; Ellingson, R.; Nozik, A. J. Multiple Exciton Generation in Colloidal Silicon Nanocrystals. *Nano Lett.* **2007**, *7*, 2506–2512.
10. Pijpers, J. J. H.; Hendry, E.; Milder, M. T. W.; Fanciulli, R.; Savolainen, J.; Herek, J. L.; Vanmaekelberg, D.; Ruhman, S.; Mocatta, D.; Oron, D.; Aharoni, A.; Banin, U.; Bonn, M. Carrier Multiplication and Its Reduction by Photodoping in Colloidal InAs Quantum Dots. *J. Phys. Chem. C* **2007**, *111*, 4146–4152.
11. Schaller, R. D.; Pietryga, J. M.; Klimov, V. I. Carrier Multiplication in InAs Nanocrystal Quantum Dots with an Onset Defined by the Energy Conservation Limit. *Nano Lett.* **2007**, *7*, 3469–3476.
12. Nair, G.; Bawendi, M. G. Carrier Multiplication Yields of CdSe and CdTe Nanocrystals by Transient Photoluminescence Spectroscopy. *Phys. Rev. B* **2007**, *76*, 081304-1−081304-4.
13. Ben-Lulu, M.; Mocatta, D.; Bonn, M.; Banin, U.; Ruhman, S. On the Absence of Detectable Carrier Multiplication in a Transient Absorption Study of InAs/CdSe/ZnSe Core/Shell1/Shell2 Quantum Dots. *Nano Lett.* **2008**, *8*, 1207–1211.
14. Pijpers, J. J. H.; Hendry, E.; Milder, M. T. W.; Fanciulli, R.; Savolainen, J.; Herek, J. L.; Vanmaekelberg, D.; Ruhman, S.; Mocatta, D.; Oron, D.; *et al*. Carrier Multiplication and Its Reduction by Photodoping in Colloidal InAs Quantum Dots. *J. Phys. Chem. C* **2008**, *112*, 4783–4784.
15. Nair, G.; Geyer, S. M.; Chang, L.-Y.; Bawendi, M. G. Carrier Multiplication Yields in PbS and PbSe Nanocrystals Measured by Transient Photoluminescence. *Phys. Rev. B* **2008**, *78*, 125325−1125325−10.
16. Trinh, M. T.; Houtepen, A. J.; Schins, J. M.; Hanrath, T.; Piris, J.; Knulst, W.; Goossens, A. P. L. M.; Siebbeles, L. D. A. In Spite of Recent Doubts Carrier Multiplication Does Occur in PbSe Nanocrystals. *Nano Lett.* **2008**, *8*, 1713–1718.
17. McGuire, J. A.; Joo, J.; Pietryga, J. M.; Schaller, R. D.; Klimov, V. I. New Aspects of Carrier Multiplication in Semiconductor Nanocrystals. *Acc. Chem. Res.* **2008**, *41*, 1810–1819.
18. Schaller, R. D.; Sykora, M.; Jeong, S.; Klimov, V. I. High-Efficiency Carrier Multiplication and Ultrafast Charge Separation in Semiconductor Nanocrystals Studied *via* Time-Resolved Photoluminescence. *J. Phys. Chem. B* **2006**, *110*, 25332–25338.
19. Allan, G.; Delerue, C. Fast Relaxation of Hot Carriers by Impact Ionization in Semiconductor Nanocrystals: Role of Defects. *Phys. Rev. B* **2009**, *79*, 195324-1–195324-5.
20. Gooding, A. K.; Gomez, D. E.; Mulvaney, P. The Effects of Electron and Hole Injection on the Photoluminescence of CdSe/CdS/ZnS Nanocrystal Monolayers. *ACS Nano* **2008**, *2*, 669–676.
21. Schaller, R. D.; Klimov, V. I. Non-Poissonian Exciton Populations in Semiconductor Nanocrystals *via* Carrier Multiplication. *Phys. Rev. Lett.* **2006**, *96*, 097402-1−097402-4.
22. Efros, A. L.; Efros, A. L. Interband Absorption of Light in a Semiconductor Sphere. *Sov. Phys. Semicond.* **1982**, *16*, 772–775.
23. Madelung, O.; Schulz, M.; Heiss, H *Numerical Data and Functional Relationships in Science and Technology, New Series*; Springer-Verlag: New York, 1982; Vol. 17, Subvol. a, p 299.
24. Klimov, V. I.; Mikhailovsky, A. A.; McBranch, D. W.; Leatherdale, C. A.; Bawendi, M. G. Quantization of Multiparticle Auger Rates in Semiconductor Quantum Dots. *Science* **2000**, *287*, 1011–1013.
25. Wang, L.-W.; Califano, M.; Franceschetti, A.; Zunger, A. Pseudopotential Theory of Auger Processes in CdSe Quantum Dots. *Phys. Rev. Lett.* **2003**, *91*, 056404-1−056404-4.
26. Lee, S.; Kim, J.; Jönsson, L.; Wilkins, J. W.; Bryant, G. W.; Klimek, G. Many-Body Levels of Optically Excited and Multiply Charged InAs Nanocrystals Modeled by Semiempirical Tight Binding. *Phys. Rev. B* **2002**, *66*, 235307-1–235307-12.
27. Puangmali, T.; Califano, M.; Harrison, P. Interband and Intraband Optical Transitions in InAs Nanocrystal Quantum Dots: A Pseudopotential Approach. *Phys. Rev. B* **2008**, *78*, 245104-1–245104-10.
28. Wang, L.-W.; Zunger, A. Local-Density-Derived Semiempirical Pseudopotentials. *Phys. Rev. B* **1995**, *51*, 17398–17416.
29. Delerue, C.; Lannoo, M.; Allan, G. Concept of Dielectric Constant for Nanosized Systems. *Phys. Rev. B* **2003**, *68*, 115411-1–115411-4.
30. Cartoixa, X.; Wang, L.-W. Microscopic Dielectric Response Functions in Semiconductor Quantum Dots. *Phys. Rev. Lett.* **2005**, *94*, 236804-1–236804-4.
31. For detailed expressions of the Auger integrals see ref 25.
32. Htoon, H.; Hollingsworth, J. A; Dickerson, R.; Klimov, V. I. Effect of Zero- to One-Dimensional Transformation on Multiparticle Auger Recombination in Semiconductor Quantum Rods. *Phys. Rev. Lett.* **2003**, *91*, 227401-1–227401-4.
33. Pandey, A.; Guyot-Sionnest, P. Multicarrier Recombination in Colloidal Quantum Dots. *J. Chem. Phys.* **2007**, *127*, 111104-1–111104-4.
34. Califano, M. Unpublished work.

35. Puangmali, T.; Califano, M.; Harrison, P. The Effect of Small Elongations on the Electronic and Optical Signatures in InAs Nanocrystal Quantum Dots. *J. Phys.: Condens. Matter* **2009**, *21*, 144212-1–144212-5.
36. Banin, U.; Lee, C. J.; Guzelian, A. A.; Kadavanich, A. V.; Alivisatos, A. P.; Jaskolski, W.; Efros, Al. L.; Rosen, M. Size-Dependent Electronic Level Structure of InAs Nanocrystal Quantum Dots: Test of Multiband Effective Mass Theory. *J. Chem. Phys.* **1998**, *109*, 2306–2309.
37. Banin, U.; Cao, Y. W.; Katz, D.; Millo, O. Identification of Atomic-like Electronic States in Indium Arsenide Nanocrystal Quantum Dots. *Nature* **1999**, *400*, 542–544.
38. Krapf, D.; Kan, S. H.; Banin, U.; Millo, O; Sa, A. Intersublevel Optical Transitions in InAs Nanocrystals Probed by Photoinduced Absorption Spectroscopy: The Role of Thermal Activation. *Phys. Rev. B* **2004**, *69*, 073301-1−073301-4.
39. Guzelian, A. A.; Banin, U.; Kadavanich, A. V.; Peng, X.; Alivisatos, A. P. Colloidal Chemical Synthesis and Characterization of InAs Nanocrystal Quantum Dots. *Appl. Phys. Lett.* **1996**, *69*, 1432–1434.
40. As it was argued in the text that in core-only NCs the presence of hole trap states at the surface leads to a negligibly small τ_h^{-1}, hence $\tau_{XX} \approx \tau_e$, the values of τ_X^+/τ_{XX} relative to these structures are not included in the inset, and $\tau_X^-/\tau_{XX} = 3$ for all core-only NCs (see Method section).
41. Puangmali, T.; Califano, M.; Harrison. P. Unpublished work.
42. Wei, S.; Zunger, A. Calculated Natural Band Offsets of All II of Cation d Orbitals. *Appl. Phys. Lett.* **1998**, *72*, 2011–2013.
43. Cao, Y. W.; Banin, U. Growth and Properties of Semiconductor Core/Shell Nanocrystals with InAs Cores. *J. Am. Chem. Soc.* **2000**, *122*, 9692–9702.
44. Although both states are contributed to by several different angular momentum components, the transition from (VBM, VBM-1), having prevalent p symmetry, to the CBM (strongly s in character) has a small oscillator strength (is formally optically forbidden) compared to the transition from (VBM-2, VBM-3), with prevalent s symmetry, to the same state. Therefore the absorption of light occurs from the optically allowed transition (VBM-2, VBM-3) → CBM, whereas emission occurs from the "dark" band edge recombination (VBM, VBM-1) → CBM, weakly allowed due to the presence of some s component in the mixed (VBM, VBM-1) state. The slow radiative recombination observed in InAs/CdSe NCs has indeed been attributed[11] to the involvement of a low-lying, optically passive dark exciton state.
45. Jha, P. P.; Guyot-Sionnest, P. Trion Decay in Colloidal Quantum Dots. *ACS Nano* **2009**, *3*, 1011–1015.
46. Shabaev, A.; Efros, A. L.; Nozik, A. J. Multiexciton Generation by a Single Photon in Nanocrystals. *Nano Lett.* **2006**, *6*, 2856–2863.
47. Franceschetti, A.; An, J. M.; Zunger, A. Impact Ionization Can Explain Carrier Multiplication in PbSe Quantum Dots. *Nano Lett.* **2006**, *6*, 2191–2195.
48. Califano, M. Efficient Auger Electron Cooling in Seemingly Unfavorable Configurations: Hole Traps and Electrochemical Charging. *J. Phys. Chem. C* **2008**, *112*, 8570–8574.
49. An, J. M.; Califano, M.; Franceschetti, A.; Zunger, A. Excited-State Relaxation in PbSe Quantum Dots. *J. Chem. Phys.* **2008**, *128*, 164720-1–164720-7.
50. Delerue, C.; Allan, G. Influence of Electronic Structure and Multiexciton Spectral Density on Multiple-Exciton Generation in Semiconductor Nanocrystals: Tight-Binding Calculations. *Phys. Rev. B* **2008**, *77*, 125340-1–125340-10.
51. When the state $|e_i,h_j\rangle$ undergoes DCM it can decay either into $|e_1,e_k;h_j,h_m\rangle$ or $|e_i,e_k;h_1,h_m\rangle$ but not into $|e_i,e_k;h_n,h_m\rangle$ if $l,k \neq i$ and $n,m \neq j$. The biexcitonic DOS that satisfy the Coulomb selection rule are effectively calculated as $\rho_{XX} = 2(\rho_X^- + \rho_X^+)$, that is, by taking the sum of the DOS relative to negative and positive trions. The factor 2 accounts for the degeneracy due to the missing fourth particle which is the fixed *spectator* carrier in both the DCM and AR processes.
52. Califano, M.; Zunger, A.; Franceschetti, A. Efficient Inverse Auger Recombination at Threshold in CdSe Nanocrystals. *Nano Lett.* **2004**, *4*, 525–531.
53. Califano, M.; Zunger, A.; Franceschetti, A. Direct Carrier Multiplication Due to Inverse Auger Scattering in CdSe Quantum Dots. *Appl. Phys. Lett.* **2004**, *84*, 2409–2411.
54. Luo, J.-W.; Franceschetti, A.; Zunger, A. Carrier Multiplication in Semiconductor Nanocrystals: Theoretical Screening of Candidate Materials Based on Band-Structure Effects. *Nano Lett.* **2008**, *8*, 3174–3181.
55. Califano, M. Model-Independent Determination of the Carrier Multiplication Time Constant in CdSe Nanocrystals. *Phys. Chem. Chem. Phys.*, in press.
56. Rabani, E.; Baer, R. Distribution of Multiexciton Generation Rates in CdSe and InAs Nanocrystals. *Nano Lett.* **2008**, *8*, 4488–4492.